PROCEEDINGS OF SCIENCE

Determination of $\Lambda^{\overline{\text{MS}}}$ from the gluon and ghost propagators in Landau gauge

André Sternbeck[*†]
Institut für Theoretische Physik, Universität Regensburg, D-93040 Regensburg, Germany
E-mail: andre.sternbeck@ur.de

Kim Maltman
Department of Mathematics and Statistics, York Univ., Toronto, ON, M3J 1P3, Canada
CSSM, School of Chemistry and Physics, University of Adelaide, SA 5005, Australia

Michael Müller-Preussker
Humboldt-Universität zu Berlin, Institut für Physik, D-12489 Berlin, Germany

Lorenz von Smekal
Institut für Kernphysik, Technische Universität Darmstadt, D-64289 Darmstadt, Germany

We give an update on our lattice determination of $r_0\Lambda_{\overline{\text{MS}}}$ for different N_f. Our calculations employ the strong coupling constant in the minimal MOM scheme for QCD in Landau gauge, and we report here on our progress towards a quantitative understanding of the intrinsic lattice discretization artifacts at large momenta. This is important for a high-precision analysis, in particular for the unquenched calculations for which the access to small lattice spacings is restricted by the available gauge configurations.

The 30 International Symposium on Lattice Field Theory – Lattice 2012,
June 24-29, 2012
Cairns, Australia

[*]Speaker.
[†]Supported by the EU commission (IRG 256594).

PoS(Lattice 2012)243

1. Introduction

Lattice Monte Carlo calculations of the strong coupling constant $\alpha_s = g^2/4\pi$ have been the subject of considerable interest in the lattice community (see figure). Over the years different schemes have been devised and lattice calculations greatly improved, to the point that the recent world average is dominated by lattice results [1].

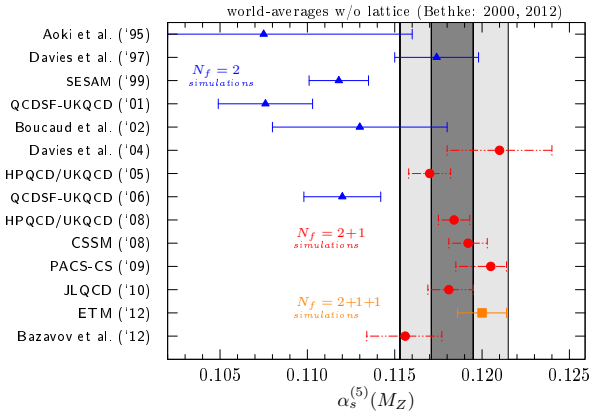

Figure 1: Lattice results for $\alpha_s^{\overline{\rm MS}}(M_Z)$. Gray bars in the background mark the non-lattice averages from 2000 and 2012 by Bethke (see, e.g., [1])

Values for α_s are traditionally given at the Z-Boson mass in the $\overline{\rm MS}$ scheme for $N_f = 5$ fermion flavors. Alternatively, one may quote, e.g., the $\overline{\rm MS}$ version of the dimensionful QCD Λ parameter, $\Lambda_{\overline{\rm MS}}^{(N_f=5)}$. The latter is often adopted when quoting $N_f = 0, 2$ lattice results. While schemes other than $\overline{\rm MS}$ must be used on the lattice, a 1-loop calculation suffices to yield $\Lambda_{\overline{\rm MS}}^{(N_f)}$ for different N_f in terms of the corresponding $\Lambda^{(N_f)}$ in these other schemes.

In 2007 [2] we introduced a method for determining $\Lambda_{\overline{\rm MS}}^{(N_f)}$ using only Landau gauge gluon and ghost propagators. These 2-point functions are easily accessible on the lattice and a product of the gluon and ghost dressing functions, Z_D and Z_G, defines the strong coupling constant [3]

$$\alpha_s^{\rm MM}(p) = \frac{g_0^2(a)}{4\pi}\, Z_D(p,a)\, Z_G^2(p,a) \qquad (\text{for } a \to 0) \tag{1.1}$$

whose running at large scales (momenta) p is known up to 4-loop order [4]. In Eq. (1.1), g_0^2 is the lattice coupling at lattice spacing a and the suffix MM refers to the Minimal MOM scheme, the underlying renormalization scheme of this coupling [4]. Note that $\alpha_s^{\rm MM}(p)$ is defined also beyond Landau gauge. The first four β-function coefficients, $\beta_0, \ldots, \beta_3$, can be found for general covariant gauges in [4]. Meanwhile this coupling has also been used by a French-Spanish collaboration [5] to estimate $\Lambda_{\overline{\rm MS}}^{(N_f)}$ and a dimension-2 gluon condensate for different N_f.

2. Simulation details

Our data for $\alpha_s^{\rm MM}$ is obtained on $N_f = 0, 2$ and $2+1$ SU(3) gauge field configurations. The quenched data is used to help quantify systematic errors, primarily due to finite volume and lattice discretization effects. $N_f = 0$ configurations are thus generated (using the standard Wilson gauge action) for different lattice spacings between $a/r_0 = 0.186$ ($\beta = 6.0$) and $a/r_0 = 0.037$ ($\beta = 7.2$), and, simultaneously, for different physical volumes L^4. We chose $L/r_0 \approx 2.5, 3.3$ and 4.3, and the r_0/a values from [6]. With our lattice spacings we cover a large range of momenta, reaching well into the perturbative regime (see below). This will allows us to fix $r_0\Lambda_{\overline{\rm MS}}^{(0)}$ free of assumptions on the source of deviations from pure 4-loop running at small momenta.

The unquenched configurations are kindly provided by the QCDSF collaboration. For $N_f = 2$ these are for the Wilson gauge action supplemented by clover-improved Wilson fermions, while

the $N_f = 2+1$ configurations are for a (tree-level) Symanzik improved gauge action and SLink fermions (see [7] for details).

All gauge configurations are fixed to lattice Landau gauge using an iterative gauge-fixing algorithm. To guarantee high-precision the local violation of transversality is not allowed to exceed $\varepsilon < 10^{-10}$ where, as usual, $\varepsilon \equiv \max_x \Re\mathfrak{e}\,\mathrm{Tr}\left[(\nabla_\mu A_{x\mu})(\nabla_\mu A_{x\mu})^\dagger\right]$ and $A_{x\mu} \equiv \frac{1}{2iag_0}(U_{x\mu} - U_{x\mu}^\dagger)|_{\text{tr.less}}$.

Standard techniques are also applied to calculate the gluon and ghost propagators. Their dressing functions are extracted, as usual, by using the exact tree-level structures of the respective lattice propagators. To reduce lattice discretization artifacts further, we consider data only for diagonal lattice momenta (strictest cylinder cut). Finally, data points for different β (and κ) are brought onto the common scale $r_0^2 p^2$, using the respective r_0/a values. For $N_f = 0$ we use the r_0/a values from [6] and for $N_f = 2$ the (new) chirally-extrapolated values from QCDSF [8].[1] For $N_f = 2+1$ we currently have data only for $\beta = 5.50$ for which $r_0/a \approx 6.59$ [9].

3. Quantifying the lattice corrections at large momenta

Though the above standard tricks nicely smoothen the momentum dependence of our α_s^{MM} data, we cannot expect it to follow exactly the continuum 4-loop running, since, even away from lower momenta where nonperturbative effects (and further down finite-volume effects) become important, corrections due to the hypercubic lattice symmetry will be needed. For a high-precision analysis it is essential to quantify these corrections, which disappear only in the continuum limit. In particular for our $N_f = 2$ and 2+1 calculations a quantitative understanding of these corrections is important. For them the access to sufficiently small lattice spacings is still limited by the available configurations ($a/r_0 \approx 0.15 \ldots 0.12$), and (small but systematic) deviations from the continuum 4-loop running at large momenta can be clearly seen in the data (see Figs. 3 and 4 below).

A complete removal of hypercubic lattice artifacts could be achieved using the so-called $H(4)$ method, as in [5]. An alternative method, however, yields reduced statistical and systematic uncertainties. To motivate this approach, consider the gluon and ghost dressing functions, Z_D and Z_G, in (infinite-volume) lattice perturbation theory (henceforth "LPT"). At 1-loop order, e.g., these have the form

$$Z_{D,G}(ap) = 1 + g_0^2\left[F_{D,G}(a^2p^2) + \Delta_{D,G}(ap)\right] \stackrel{a\to 0}{=} 1 + g_0^2 F_{D,G}(a^2p^2) \tag{3.1}$$

with $F_{D,G}(a^2p^2) = \left(c_{11}^{D,G}\log(a^2p^2) + c_{10}^{D,G}\right)$ the part that survives in the continuum limit. The 1-loop coefficients $c_{10}^{D,G}$ and $c_{11}^{D,G}$ are known since the eighties [10]. For the hypercubic corrections, however, we are interested in $\Delta_{D,G}(ap)$. These terms are non-zero for finite a, depend on the momentum ap and its direction $\big($with $ap_\mu = 2\pi k_\mu/N_\mu$ and $k_\mu \in (-N_\mu/2, N_\mu/2]\big)$ and represent the 1-loop contributions to the hypercubic lattice artifacts. For lattice hadron physics applications, e.g., it is common to calculate such correction terms and subtract them from the lattice data for some operators before determining the RGI scheme renormalization factors (see, e.g., [11]). Whether this removes sufficiently the bulk of lattice artifacts depends on the quantity being considered.

For the gluon and ghost propagators, to the best of our knowledge, nothing is really known about $\Delta_{D,G}(ap)$. We therefore calculated them in LPT by evaluating (mostly by numerical integration) the two Feynman diagrams (sunset and tadpole) for the ghost self-energy and another seven

[1] Note that the new r_0/a values have changed, this explains why $r_0\Lambda_{\overline{\text{MS}}}^{(2)}$ is now larger than before [2].

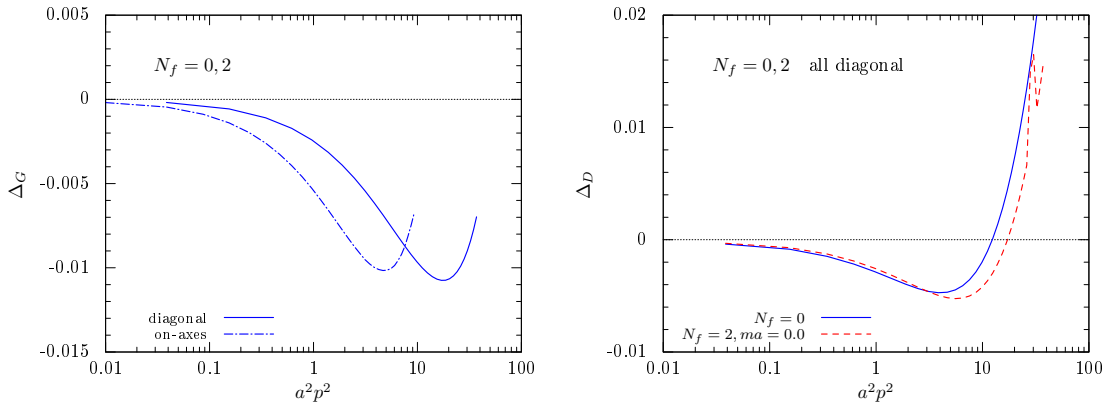

Figure 2: Hypercubic (1-loop) corrections, Δ_G (left) and Δ_D (right), versus a^2p^2. Δ_G is shown for on-axis (dash-dotted line) and diagonal momenta (solid line), while Δ_D only for diagonal momenta, but for $N_f = 0$ (solid line) and $N_f = 2$ (dashed line) massless fermions. Note that at 1-loop, Δ_G is independent of N_f.

for the gluon self-energy, all for the whole range of external momentum (ap). In particular the gluon self-energy diagrams containing 3- and 4-gluon vertices are quite cumbersome.[2]

The outcome of our 1-loop LPT calculation is shown in Fig. 2. The left panel shows $\Delta_G(ap)$ for two directions of ap, diagonal and on-axis. As expected, the hypercubic corrections grow with $|ap|$ and are smallest (but not at all zero) for diagonal ap. This is why the widely used *cylinder cuts* are so effective in removing a large fraction of the lattice artifacts from the data, though these are not removed completely. The right panel shows $\Delta_D(ap)$ for $N_f = 0$ and $N_f = 2$ massless fermions. For simplicity only diagonal momentum results are shown, the comparison of diagonal and on-axis momenta being similar to that seen for $\Delta_G(ap)$.

Looking at Fig. 2 and the definition of α_s^{MM} one sees that, to leading order, the lattice corrections to $\alpha_s^{\text{MM}}(r_0 p)$ are of the form $\alpha_s^{\text{MM}}(r_0 p) + g_0^4\,[\Delta_D(ap) + 2\Delta_G(ap)] + O(g_0^6)$. Some of the corrections to the dressing functions will thus cancel in the α_s^{MM} data at larger ap.

After subtracting $\Delta_D(ap)$ and $\Delta_G(ap)$ corrections from our data for Z_D and Z_G, we find, unfortunately, only minor reductions in the size of lattice artifacts. Higher-loop corrections are thus needed, but calculations beyond 1-loop LPT are not feasible because of their complexity. Within the framework of Numerical Stochastic LPT this might be possible [14]. We have begun looking into this.

In any case, from this exercise we know the remaining corrections should be of the leading order $O(g_0^6)$. That is, a hypercubic Taylor expansion of the (1-loop) subtracted α_s^{MM} data for diagonal lattice momenta, denoted $\alpha_{\text{MC,sub}}^{\text{MM}}$ henceforth, should be of the form

$$\alpha_{\text{MC,sub}}^{\text{MM}}(r_0 p, ap) = \alpha_s^{\text{MM}}(r_0^2 p^2) + g_0^6\left[c_2 \cdot (ap)^2 + c_4 \cdot (ap)^4 + \ldots\right] + O(g_0^8) \qquad (3.2)$$

where c_2 and c_4 are constants. In fact, this leading-order expression describes the bulk of the lattice artifacts surprisingly well. We can fit our lattice data, $\alpha_{\text{MC,sub}}^{\text{MM}}(r_0 p, ap)$, *simultaneously* for different β with the ansatz Eq. (3.2) with only three parameters: c_2, c_4 and $r_0\Lambda_{\text{MM}}$ (resp. $r_0\Lambda_{\overline{\text{MS}}}$), where the latter parametrizes the 4-loop running of α_s^{MM} $\left(\text{resp. } \alpha_s^{\overline{\text{MS}}}\right)$ in the continuum.

[2] A.S. thanks Holger Perlt for his help and support of (many lines of) expressions for these vertices.

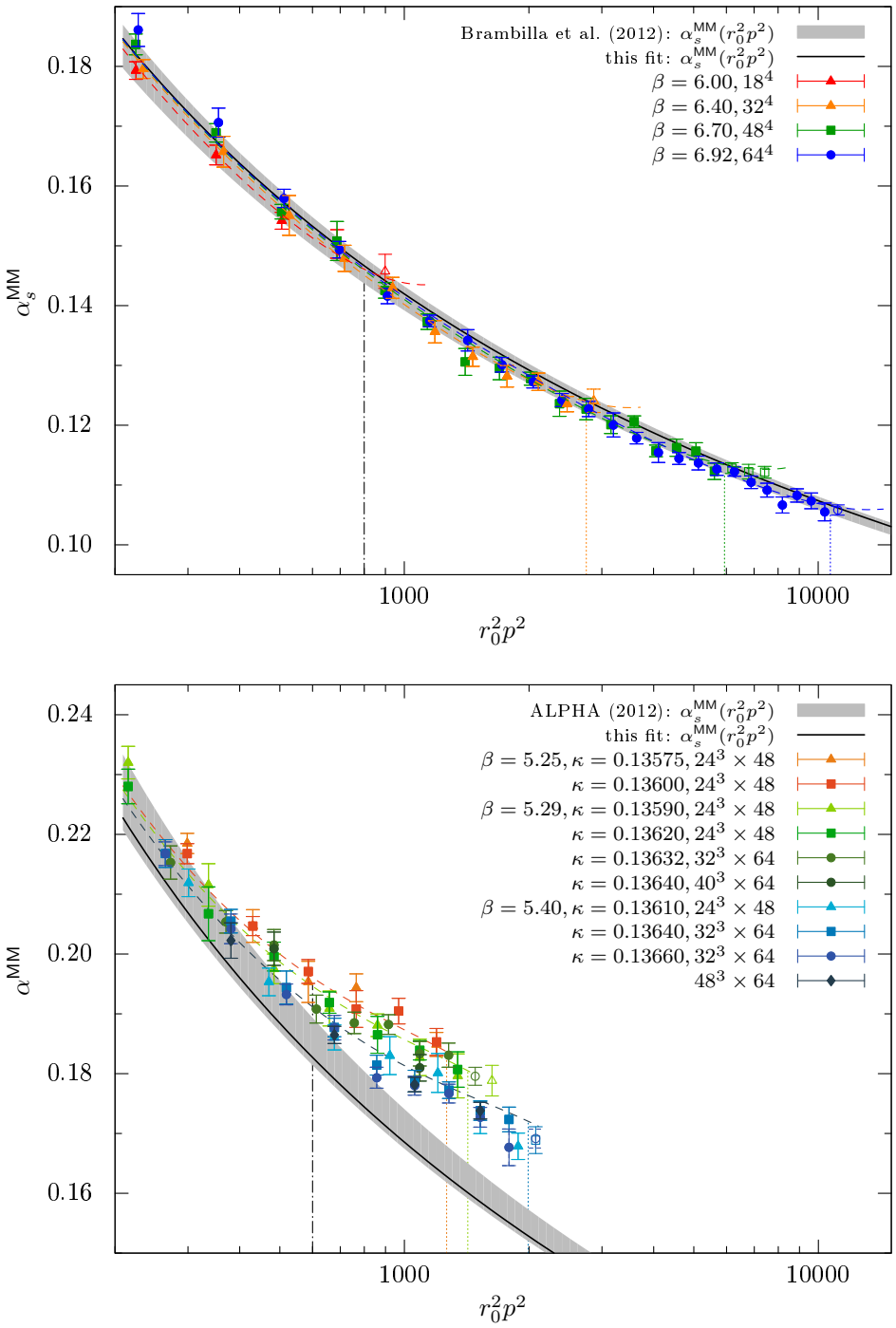

Figure 3: $\alpha^{\text{MM}}_{\text{MC,sub}}$ versus $r_0^2p^2$ for $N_f = 0$ (top) and $N_f = 2$ (bottom). The gray band is $\alpha_s^{\text{MM}}(r_0^2p^2)$ running at 4-loop using $r_0\Lambda^{(0)}_{\overline{\text{MS}}} = 0.637(32)$ and $r_0\Lambda^{(2)}_{\overline{\text{MS}}} = 0.789(52)$ as input [12, 13]. The solid line (on this band) is $\alpha_s^{\text{MM}}(r_0^2p^2)$ as it comes out from a fit of $\alpha^{\text{MM}}_{\text{MC,sub}}$ to Eq. (3.2) (no error band shown). For $N_f = 2$ all data shown has been used (simultaneously) for the fit. For $N_f = 0$ we show data for only one physical volume for simplicity, but seven more sets entered the fit. The (colored) dashed curves, connecting the data points, refer to $\alpha_s^{\text{MM}}(r_0^2p^2)$ plus the fitted lattice corrections (see Eq. (3.2)). Vertical lines mark the fit window: a dashed-dotted line marks the lower bound $r_0^2p^2_{\text{min}} = 800$ $\left(r_0^2p^2_{\text{min}} = 600 \text{ for } N_f = 2\right)$ and dotted lines the upper bound $a^2p^2_{\text{max}} = 29$. Open symbols are for points where $a^2p^2 > a^2p^2_{\text{max}}$.

4. Results

To illustrate how well ansatz (3.2) performs we show in Fig. 3 our (subtracted) $\alpha_s^{\rm MM}$ data versus $r_0^2p^2$ for $N_f=0$ (top) and $N_f=2$ (bottom), together with the curves from a global fit. A solid (black) line refers to $\alpha_s^{\rm MM}(r_0^2p^2)$, the strong coupling in the continuum at 4-loop running, while the (colored) dashed lines refer to $\alpha_s^{\rm MM}(r_0^2p^2)+g_0^6\left[c_2\cdot(ap)^2+c_4\cdot(ap)^4\right]$. Note that $g_0^2=2N_c/\beta$ varies with β, but c_2 and c_4 are the same for all data sets of same N_f. For the fit shown in Fig. 3, the fitting window starts at $r_0^2p^2=800$ ($r_0^2p^2=600$ for $N_f=2$) and ends at $a^2p^2=29$. Other fit windows give similar results, but we see first deviations from 4-loop running below $r_0^2p^2=500$. Due to the large lower bound finite-volume effects play no role. For the purpose of this illustration, we therefore fitted the data for all available volumes, and also did not distinguish the quark masses. This is suggested by the weak quark-mass (κ) dependence of our $N_f=2$ data (the corresponding pion masses are $m_\pi\approx 160\ldots720\,$MeV, see [8]). To not overload Fig. 3, the $N_f=0$ data is shown only for one physical volume.

For a comparison, we also show the continuum coupling $\alpha_s^{\rm MM}(r_0^2p^2)$ running at 4-loop (gray bands) using as input the recent values $r_0\Lambda_{\overline{\rm MS}}^{(N_f=0)}=0.637(32)$ and $r_0\Lambda_{\overline{\rm MS}}^{(N_f=2)}=0.789(52)$ from the literature [12, 13]. Our fits fully agree with these values.

As mentioned above, there is also $\alpha_s^{\rm MM}$ data for $N_f=2+1$. We are currently in the process of calculating $\alpha_s^{\rm MM}$ on all the different sets provided by QCDSF to estimate $r_0\Lambda_{\overline{\rm MS}}^{(3)}$. So far we have data only for one β (see Fig. 4) on rather course lattices ($a/r_0\approx0.15$). But a first fit, similar to those discussed above, demonstrates already good agreement with the $\Lambda_{\overline{\rm MS}}$ from [15]. This is just a first fit attempt, and a more thorough study will follow. But our new approach of dealing with the lattice corrections (via Eq. (3.2) and restricting to data with diagonal momenta) seems to work nicely. It will allow us to fix $r_0\Lambda_{\overline{\rm MS}}^{(N_f)}$, without the need to assume anything on the nature of the deviations from pure 4-loop running at smaller momenta (higher-loop corrections, dim-2 condensate, etc.) as was necessary in [5].

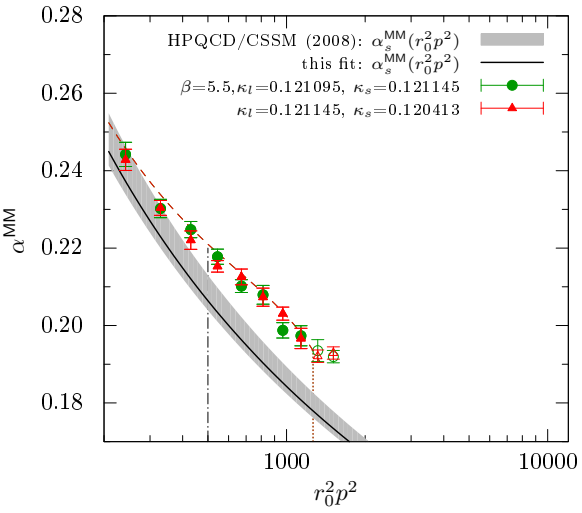

Figure 4: Two sets of our $N_f=2+1$ data and a first fit attempt similar to what was done for Fig. 3.

5. Summary

We presented an update on our determination of $r_0\Lambda_{\overline{\rm MS}}^{(N_f)}$ for different N_f. For this we use a renormalization scheme (Minimal MOM scheme in Landau gauge) that only requires lattice data for the gluon and ghost propagators in Landau gauge [4]. In this contribution we focused on a quantitative understanding of the hypercubic lattice artifacts at large momenta. This is important for a high-precision analysis, in particular for our unquenched calculations, for which the access to

momenta above 10 GeV is limited by the available gauge configurations. To make maximal use of data at large lattice momenta ($a^2p^2 \gg 1$) we determined the leading hypercubic lattice corrections to $\alpha^{\rm MM}_{\rm MC,sub}$. This was achieved by a calculation of the contribution at 1-loop order in LPT and secondly by a simultaneous fit of our lattice data (for diagonal momenta) to Eq. (3.2). It then very well describes the leading lattice corrections to $\alpha^{\rm MM}_{\rm MC,sub}$ with just three free parameters, one of which is $r_0\Lambda^{(N_f)}_{\overline{\rm MS}}$. Values for $r_0\Lambda^{(N_f)}_{\overline{\rm MS}}$ for $N_f = 0$ and $N_f = 2$ (and perhaps even $N_f = 2+1$) will be given in a forthcoming article. There we will give also more details on our data and fits, and on the LPT calculations presented above.

We are indebted to Holger Perlt for his help on getting the 1-loop LPT calculations right. This work is supported by the European Union under the Grant Agreements IRG 256594 and 249203. K.M. is supported by NSERC (Canada) and L.v.S. by the Helmholtz International Center for FAIR. We thank the HLRN (Germany) for the generous support of computing time over the years.

References

[1] S. Bethke(2012), arXiv:1210.0325 [hep-ex].
[2] A. Sternbeck *et al.*, PoS **LAT2007**, 256 (2007), arXiv:0710.2965 [hep-lat]; A. Sternbeck *et al.*, PoS **LAT2009**, 210 (2009), arXiv:1003.1585 [hep-lat].
[3] L. von Smekal, R. Alkofer, and A. Hauck, Phys.Rev.Lett. **79**, 3591 (1997), arXiv:hep-ph/9705242 [hep-ph].
[4] L. von Smekal, K. Maltman, and A. Sternbeck, Phys.Lett. **B681**, 336 (2009), arXiv:0903.1696 [hep-ph].
[5] P. Boucaud *et al.*, Phys.Rev. **D79**, 014508 (2009), arXiv:0811.2059 [hep-ph]; B. Blossier *et al.*, Phys.Rev. **D85**, 034503 (2012), arXiv:1110.5829 [hep-lat]; B. Blossier *et al.*, Phys.Rev. **D82**, 034510 (2010), arXiv:1005.5290 [hep-lat]; B. Blossier *et al.*, Phys.Rev.Lett. **108**, 262002 (2012), arXiv:1201.5770 [hep-ph].
[6] S. Necco and R. Sommer, Nucl.Phys. **B622**, 328 (2002), arXiv:hep-lat/0108008 [hep-lat]; M. Guagnelli, R. Petronzio, and N. Tantalo, Phys.Lett. **B548**, 58 (2002), arXiv:hep-lat/0209112 [hep-lat].
[7] W. Bietenholz *et al.*, Phys.Rev. **D84**, 054509 (2011), arXiv:1102.5300 [hep-lat].
[8] G. Bali *et al.*, Nucl.Phys. **B866**, 1 (2013), arXiv:1206.7034 [hep-lat].
[9] G. Bali and J. Najjar, in preparation.
[10] H. Kawai, R. Nakayama, and K. Seo, Nucl.Phys. **B189**, 40 (1981).
[11] M. Göckeler *et al.*, Phys.Rev. **D82**, 114511 (2010), arXiv:1003.5756 [hep-lat].
[12] N. Brambilla *et al.*, Phys.Rev.Lett. **105**, 212001 (2010), arXiv:1006.2066 [hep-ph].
[13] P. Fritzsch *et al.* (ALPHA Collaboration), Nucl.Phys. **B865**, 397 (2012), arXiv:1205.5380 [hep-lat].
[14] F. Di Renzo *et al.*, Nucl.Phys. **B831**, 262 (2010), arXiv:0912.4152 [hep-lat]; F. Di Renzo *et al.*, Nucl.Phys. **B842**, 122 (2011), arXiv:1008.2617 [hep-lat]; E.-M. Ilgenfritz *et al.*, Phys.Rev. **D83**, 054506 (2011), arXiv:1010.5120 [hep-lat].
[15] C. Davies *et al.* (HPQCD Collaboration), Phys.Rev. **D78**, 114507 (2008), arXiv:0807.1687 [hep-lat]; K. Maltman, D. Leinweber, P. Moran, and A. Sternbeck, Phys.Rev. **D78**, 114504 (2008), arXiv:0807.2020 [hep-lat]